Energy Management Algorithm for Resilient Controlled Delivery Grids

Mahmoud Saleh, Graduate Student *Member*, *IEEE*, Yusef Esa, Graduate Student *Member*, *IEEE*, Ahmed A. Mohamed, Haim Grebel and Roberto Rojas-Cessa

Abstract-Resilience of the power grid is most challenged at power blackouts since the issues that led to it may not be fully resolved by the time the power is back. In this paper, a Real-Time Energy Management Algorithm (RTEMA) has been developed to increase the resilience of power systems based on the controlled delivery grid (CDG) concept. In a CDG, loads communicate with a central controller, periodically sending requests for power. The central controller runs an algorithm, based on which it may decide whether to grant the requested energy fully or partially. Therefore, the CDG limits loads discretionary access to electric energy until all problems are resolved. The developed algorithm aims at granting most or all of the requested loads, while maintaining the health of the power system (i.e. the voltage at each bus, and the line loading are within acceptable limits), and minimizing the overall losses. An IEEE 30-bus standard Test Case, encountering a blackout condition, with high penetration of microgrids, has been used to test the developed algorithm. Results proved that the developed algorithm with the CDG have the potential to substantially increase the resilience of power systems.

Index Terms—Controlled delivery grid, communication based control, energy management algorithm, microgrids, microgrid clustering, resiliency.

I. Nomenclature

[<i>C</i>]	Correction matrix.				
Co	Signal that indicates whether the system is connected to the main grid (0), or there is a blackout (1).				
C_I	Constraint showing the second selection criteria of				
CI	the proposed algorithm.				
G_{ik}, B_{ik}	Real and imaginary components of Y_{ik} .				
I	The set of inputs.				
[J]	Jacobian matrix				
[M]	Mismatch matrix.				
NC	Sets of numbers of all combinations.				
NMG	Sets of numbers of the MGs within the system.				
$P_{I,I,}^{max}$	Maximum transmission line loading.				
$P_{l,i}^r, Q_{l,i}^r$					
P_s, Q_s	Calculated active and reactive powers from the load flow for the selected MG connected to the slack bus.				
THE 1 ALL ALM ALM ALCOHOLD					

This work was supported in part by the National Science Foundation under Awards 1641033 and 1640715.

Mahmoud Salah, Yusef Esa and Ahmed Mohamed are with the Department of Electrical Engineering, City College of the City University of New York, New York, NY 10031 USA (e-mail: amohamed@ccny.cuny.edu).

Haim Grebel and Roberto Rojas-Cessa are with the Department of Electrical and Computer Engineering, New Jersey Institute of Technology, Newark, NJ 07102 USA (e-mail: rojas@njit.edu).

$P_{g,i}^r, Q_{g,i}^r$	Generation active and reactive power request from bus <i>i</i> .						
P_{SL}, Q_{SL}	Active and reactive power limit of the MG connected to the slack bus.						
P_{LS}	Total power losses of the system.						
$P_{LS} _{VL}$	Aggregated power losses of the entire system associated with each combination of S_{VL} .						
S	Set of all possible solutions.						
S_{GL}	Set of solutions for granting that passed the generating limit constraint.						
\mathcal{S}_{VL}	Set of solutions that passed C_I .						
S_g	Solution satisfied all constraints.						
V_{dev}^{max}	Maximum bus voltage deviation among all the buses within the system.						
V_i, V_k	Voltages at buses i and k						

II. INTRODUCTION

RESILIENCE as articulated by Presidential Policy Directive 21 (PPD)-21 refers to "the ability to prepare for and adapt to changing conditions and withstand and recover rapidly from disruptions. Resilience includes the ability to withstand and recover from deliberate attacks, accidents, or naturally occurring threats or incidents" [1]-[5]. The ever-increasing dependence on electricity in current societies makes the power grid one of the most critical infrastructures. The recent series of severe storms that have caused massive and extended power outages affecting millions of people in the mid-Atlantic and Northeast regions of the USA, and causing billions of dollars of economic losses, has triggered the imperative to explore new approaches to increase the power grid resilience [6]-[8].

Inspecting how previous blackouts initiated, and how a few contingencies caused cascaded failures that propagated throughout the power grid, a major reason for blackouts, in our view, is loads discretionary access to electric power. For a stable power system, at any given instant, the total power produced by all the generators must equal the total power demanded by the loads, in addition to the power lost during the power transmission and distribution stages. While power system operators have control over the generation, they have very limited control over the loads. In other words, loads can draw power at any time as long as they are connected to the power grid. Historically, this critical load/generation balance has been achieved through frequency signaling –that is using frequency deviation from the nominal 60 Hz to signal load/generation unbalance.

Since all generators within an interconnected power grid are precisely synchronized, frequency is a global characteristic that can be measured at any bus. An under-frequency condition (i.e. less than 60 Hz) implies that generators need to produce more power, while over-frequency means that they need to produce less. This operational philosophy has the advantage of controlling the power grid with minimal dependence on realtime feedback from loads and consequently less dependence on communication networks. However, it is likely to fail under heavy loading conditions, such as those experienced in hot summer days. Moreover, it almost always fails under severe contingencies, such as those resulting from weather-driven events. Load shedding represents a means for operators to reduce the total demand, by coarsely cutting some feeders during emergencies. This helps confine some of the failures. However, load shedding in some occasions may aggravate the problem, and it cannot guarantee prevention of further cascaded failures.

The Controlled Delivery Grid (CDG) concept has been developed by Grebel and Rojas-Cessa in [9], [10]. The CDG challenges the common wisdom of passively responding to arbitrary load changes, and depending minimally on communication networks for power grid operation. It suggests full real-time monitoring and control of the loads. A controlled delivery grid is overlaid with a data network that communicates with every load on the network. Loads communicate with a central controller, periodically sending "requests" for power. The central controller processes all the requests, and yield back "grants." Loads may or may not be granted the power that they requested.

While the CDG can potentially result in major enhancement in several power grid operational functions, such as service restoration, this paper will be focused on the impact of CDG on power grid resilience. We hypothesize that a CDG can substantially increase the resilience of a power grid; a controller will run an algorithm to process the load requests, and only grant power after evaluating, ahead of time, the impact of the loads. Therefore, theoretically, the possibility for a blackout is minimal. In order to test this hypothesis, we have developed an energy management algorithm to process load requests, and implemented it on a power grid with finite generation capability and multiple microgrids.

Previous research on energy management algorithms either focused on small scale systems like microgrids [11]- [13], or distribution systems with electrical vehicles [14], [15]. Others used game theory to analyze economically the energy transfer between distributed generations within a smart distribution system [16]. In this paper, a real-time energy management was implemented in a modified IEEE 30-bus distribution system with high penetration of microgrids. It was developed adopting the CDG concept to increase the resilience of the system.

The rest of the paper is organized as follows. In section II, the power grid used as a case study in this paper will be presented. In section III, the developed real-time energy management algorithm (RTEMA) will be described. In section IV, the results of implementing the developed RTEMA on the example power grid have been presented and discussed.

TABLE I

LC	_				
	Level 1	Level 2	Level 3	Level 4	{(1,1),(1,1),(1,1)}
	P,Q (p.u.)	P,Q (p.u.)	P,Q (p.u.)	P,Q (p.u.)	{(1, 1), (1, 1), (0.7, 0.7)}
Area 1	1,1	0.8, 0.8	0.5, 0.5	0.4, 0.4	{(1, 1), (0.75, 0.75),
Area 2	1,1	0.75, 0.75	0.45, 0.45	0.3, 0.3	(0.7, 0.7)}
Area 3	1,1	0.7, 0.7	0.4, 0.4	0.3, 0.3	{(0.4, 0.4), (0.3, 0.3), (0.3, 0.3)}

Finally, in section V, some of the conclusions that can be derived from this paper will be summarized.

III. SYSTEM UNDERSTUDY

The system understudy is shown in Fig. 1. It represents the IEEE 30-bus standard Test Case. The bus and line data have been extracted from [17]. The system has been modified to represent a blackout condition, by disconnecting the main infeed coming from generator 1. The system is divided into three load areas, namely Area 1, Area 2 and Area 3. The loads at each area follow a different profile as shown in Fig. 1. These load profiles were adapted from actual load patterns of three regions in New York State: Mohawk Valley, Long Island, and New York City [18].

The total demand is 283.4 MW of active power, and 126.2 MVar of reactive power. We assume that three microgrids are connected to the system, at buses 3, 5 and 10. The rated apparent power, $\{P_i, Q_i\}$, for these three microgrids are $\{80 \text{ MW}, 50 \text{ MVar}\}$, $\{80 \text{ MW}, 30 \text{ MVar}\}$ and $\{50 \text{ MW}, 20 \text{ MVar}\}$. Bus 3 was chosen to connect microgrid 1 (MG1) to be close to the slack bus. Bus 5 was chosen to connect MG2 to be close to the dense load area. Bus 10 was arbitrarily chosen to connect MG3.

Each bus has a local controller. These controllers, in the case of load buses, send load requests $(P_{l,i}^r)$, where subscript l means "load" and i denotes the bus number) to the control center that runs the RTEMA. In the case of microgrid buses, these local controllers represent the Microgrid Central Controllers (MGCC), and send generation requests $(P_{g,i}^r)$. In other words, loads send requests asking to receive power for the next time step, while microgrids ask for a permission to inject a certain amount of active and reactive power. Microgrids can also request power if needed.

For each time step, the control center aggregates all the requests, and attempts to grant 100% of the total requested load, i.e. it runs the algorithm to find a solution that satisfies all the constraints with all requested loads granted. If no feasible solution exists, the algorithm has to search for a solution with some requests not being fully granted. The grant reduction decision may be based on a priority list.

In this paper, we assume that each bus controller will send a load request, in the form of a set that contains four load levels, with a minimum of 10% difference as shown in Table I. The three load areas of the 30-bus system have different load-serving priorities, such that Area 1 has the highest priority, followed by Area 2, followed by Area 3. The control center will attempt to grant all the requested loads. If it fails to do so, it will repeat the algorithm for a reduced load, based on their priorities, as shown in Table I.

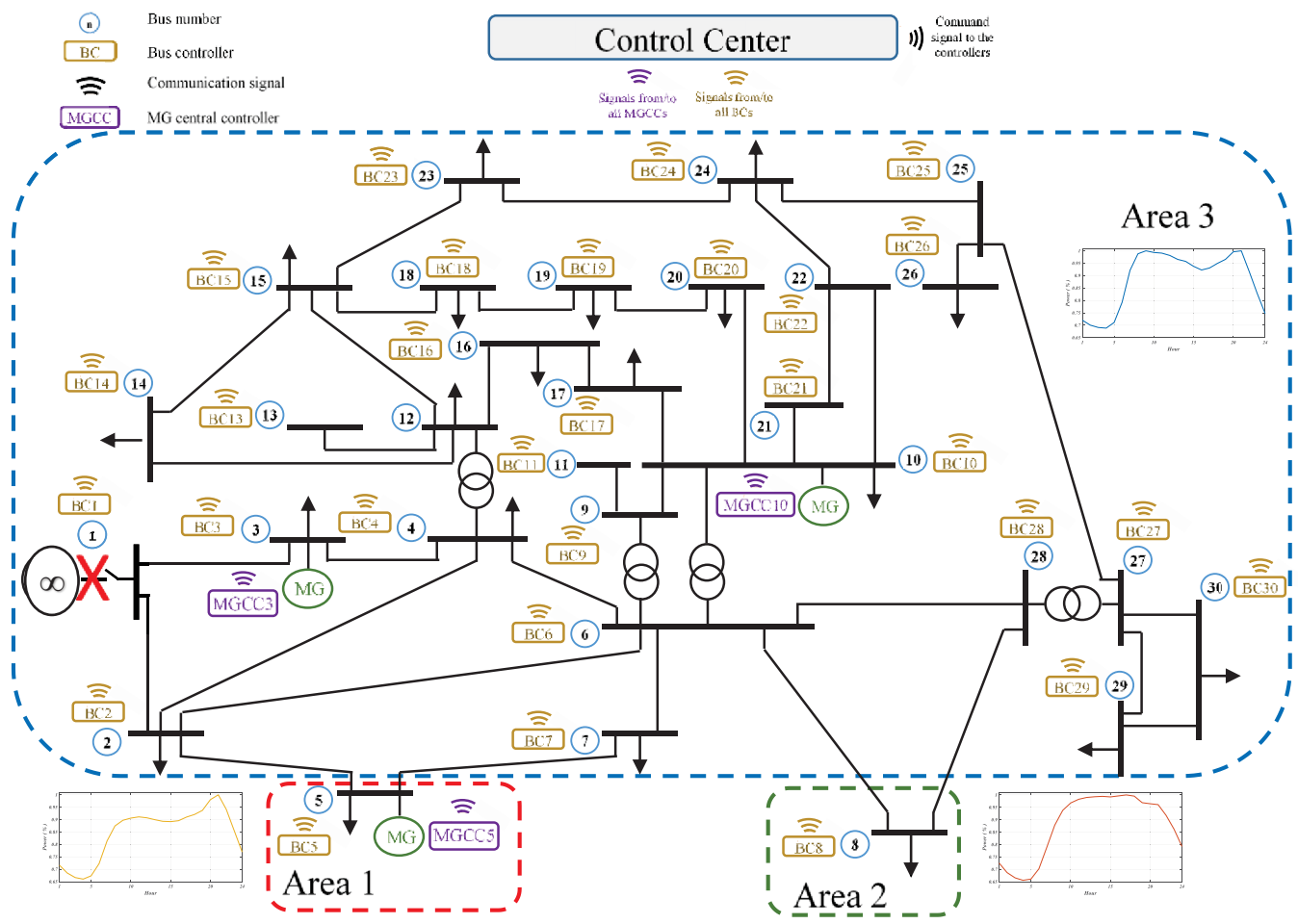


Fig. 1. The modified IEEE 30-bus Test Case.

IV. REAL-TIME ENERGY MANAGEMENT ALGORITHM

The proposed RTEMA processes all the load and power injection requests. It searches for an optimal solution, and yield grants to the loads to consume energy, or to the microgrids to inject power. Requests may be fully or partially granted depending on the state of the power system, which is determined by iteratively solving the load flow problem using the Newton Raphson method. The active and reactive power are calculated in rectangular coordinates using (1) and (2), respectively,

$$P_{i} = \sum_{k=1}^{n} |V_{i}| |V_{k}| (G_{ik} \cos \theta_{ik} + B_{ik} \sin \theta_{ik})$$
 (1)

$$Q_{i} = \sum_{k=1}^{n} |V_{i}| |V_{k}| (G_{ik} \sin \theta_{ik} - B_{ik} \cos \theta_{ik})$$
 (2)

Where G_{ik} and B_{ik} are the real and imaginary components of Y_{ik} (the element at the i^{th} row, k^{th} column of the Y_{bus}), θ_{ik} is the angle of Y_{ik} .

A load flow solution is achieved by minimizing mismatches between the calculated and specified values of P_i at load (P-Q)and voltage-controlled (P-V) buses, and Q_i at the P-Q buses. The Jacobian matrix (J), in (3), is calculated to relate the mismatches, to corrections in the unknown quantities (Newton

Raphson variables), which are the voltage magnitude $|V_i|$ and angle δ_i at P-Q buses, and angles only at P-V buses.

$$[M]^{(v)} = [J]^{(v)}[C]^{(v)}$$
(3)

Where v denotes the iteration number, [M] is the mismatches matrix, [J] is the Jacobian matrix, and [C] is the correction matrix.

Once it receives requests, the developed RTEMA runs the load flow assuming that all loads will be granted. It then sequentially eliminates unacceptable results based on predefined constraints. The output is the amount of power granted to each load, and the power injection (set points) from each microgrid.

This can be represented as,

minimize
$$\sum_{i=1}^{NB} \left(P_{l,i}^r - P_{l,i}^g \right) \tag{4a}$$

subject to
$$P_i^g = \sum_{\substack{k=1 \ NB}}^{NB} |V_i| |V_k| (G_{ik} \cos \theta_{ik} + B_{ik} \sin \theta_{ik})$$
 (4b)

$$Q_i^g = \sum_{k=1}^{NB} |V_i| |V_k| (G_{ik} \sin \theta_{ik} - B_{ik} \cos \theta_{ik})$$
 (4c)

$$P_{g,i}^g \le P_{g,i}^r \tag{4d}$$

$$P_{g,i}^{g} \le P_{g,i}^{r}$$

$$(4d)$$

$$C_{l} = (|V|^{min} \le |V_{dev}^{max}| < |V|^{max}) &&(P_{LL} < P_{L})$$

$$(4e)$$

Algorithm I depicts the operation of the proposed RTEMA

during normal operation or in case of blackout. The multilayer decision Algorithm encompasses several selection phases including: maximum generation limits, maximum bus voltage deviation, maximum line loading and the least system losses.

Algorithm I: Real Time Energy management
Algorithm

```
Input:
               Load and power injection requests P_{q,i}^r, Q_{q,i}^r, P_{l,i}^r and
                               time
                                          step,
                                                     such
                                                                that
                                                                        (\forall I
               NB)(\{P_{g,i}^r, Q_{g,i}^r, P_{l,i}^r, Q_{l,i}^r\} \in I)
              Set of (P_{g,i}^g, Q_{g,i}^g) in S_g \in S
       if C_0 = 1 then
            for k \leftarrow 1 to NMG do
                   Select MG_k to be the slack
                        for n \leftarrow 1 to \forall c \ (c \neq k \rightarrow \exists S_c \in CB) do
                           Solve load flow for S_c
                             if P_s < P_{SL} && Q_{SL} then
                                S_c \in S_{GL}
                             end if
                         end for
            end for
            if S_{GL} = \{\emptyset\} then
            repeat with the next level of load request
            end if
            for each combination in S_{GL}
                   if C_1 = 1 then
                          S_c \in S_{VL}
                   end if
            end for
            if S_{VL} = \{\emptyset\} then
            repeat with the next level of load request
            end if
           P_{LS} \leftarrow any of the combination \in S_{VL}
            for each combination in S_{VL} do
                       if P_{LS}|_{VL} < P_{LS}
                          P_{LS} \leftarrow P_{LS}|_{VL}
                          S_c \in S_g
                       end if
            end for
       else
             for j \leftarrow 1 to NC do
                Solve for the load flow for S_c
                           if C_1 = 1 then
                              S_c \in S_{VL}
                           end if
             end for
             if S_{VL} = \{\emptyset\} then
             repeat with the next level of load request
             P_{LS} \leftarrow any of the combination \in S_{VL}
             for each combination in S_1 do
                           if P_{LS}|_{VL} < P_{LS}
                               P_{LS} \leftarrow P_{LS}|_{VL}
                               S_c \in S_g
                            end if
       end for
       Return S_{g}
```

V. RESULTS AND DISCUSSION

The operation of the proposed energy management algorithm has been tested using the modified IEEE 30-bus system described in Section III. The system is experiencing a blackout condition, since the main infeed from bus 1 is disconnected. We will analyze how the CDG with the proposed algorithm enable the microgrids to re-energize the power grid, supplying the loads. The various bus controllers send load requests based on the profiles shown in Fig. 1. Figures 2 and 3 show the sequential search procedure of the algorithm for an optimal solution, for 7:00am and 9:00pm, respectively. These two hours were arbitrarily chosen to depict the operation of the algorithm during off-peak and peak times. The first, second and third rows in Figs. 2 and 3 show the algorithm results for the cases when buses 3, 5 and 10 are considered the slack bus, respectively. The x-axis in all subplots of Figs. 2 and 3 represent the combined apparent power from all microgrids except the one connected to the slack bus. The y-axis in the first, second and third columns in Figs. 2 and 3 represent the active power of the microgrid connected to the slack bus, the maximum line loading, and the maximum voltage deviation, respectively. The red dashed line in each subplot of Figs. 2 and 3 represents the passing threshold for the algorithm results. The red circles represent the rejected solutions, while the blue circles represent the acceptable ones. The focus in the graphs is on the active power because it was observed that the reactive power within acceptable limits.

As shown in Fig. 2a, at 7:00am, some solutions were acceptable (marked with the blue circles), since the power of the microgrid connected to the slack bus is below its limit (i.e. $P_S < P_{SL}$ in Algorithm I). Note that we check the power limit of the microgrid connected to the slack bus only, since the other two microgrids will receive generation set points within their acceptable limits. Fig. 2d shows the solutions with respect to line loading (the limit was chosen to be 80%). It can be seen that some solutions were exceeding the permissible limit, while other solutions were acceptable. Fig. 2g shows the algorithm results with respect to maximum voltage deviation. It can be observed that all the results through this phase are within acceptable voltage limits. Finally, among the solutions that pass all the three selection phases, the one that results in the minimum overall losses is chosen. It should be noted that all the load requests were granted during this hour since the total load is not high (i.e. off-peak hour).

Similarly, Fig. 3 shows the selection process at 9:00pm. However, in this case, since the requested load is relatively high, the algorithm cannot find a feasible solution if it grants all the load requests. It recursively searches for a solution, until it finds one when it grants 80%, 75% and 40% of the requested loads at Area 1, Area 2 and Area 3, respectively. According to Table I, the algorithm had to go through five loops of load reduction, since the aggregate load requested is higher than the total generation from all microgrids.

Figures 4a, 4b and 4c shows the normalized requested load, and the normalized granted power for 24 hours at Areas 1, 2 and 3, respectively. The number of the bus chosen by the algorithm to be the slack bus is presented at each hour. It can be observed that all the requested loads are granted during the early hours when the load is low. As the load increases, the gap between the

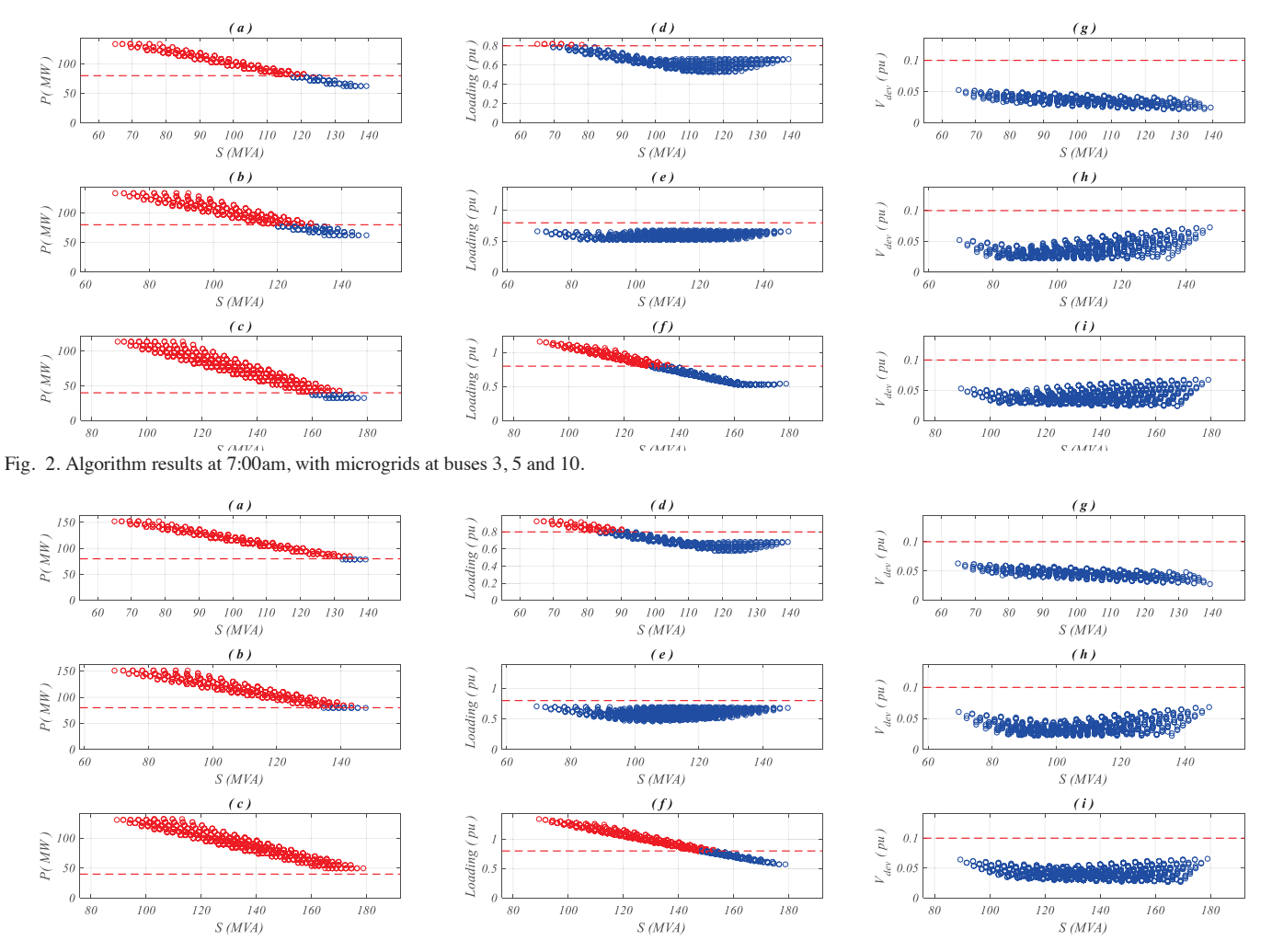


Fig. 3. Algorithm results at 9:00pm, with microgrids at buses 3, 5 and 10.

two curves increases showing that less requests are being granted. It can also be observed that Area 1 has the highest ratio of granted power over requested load, as compared to Areas 2 and 3 since it has the highest priority throughout the day, as described in Table I. It can also be noted that as the load changes in the three areas, the algorithm decides which microgrid bus will serve as the slack bus, such that all the constraints described in Algorithm I are satisfied, and the total losses are minimum. At 4:00pm, the requested load from Area 1 slightly decreased allowing Area 3 to be granted more power. It can also be seen that the algorithm chose the microgrid connected to bus five to be the slack bus.

In order to study the impact of the microgrid location on the operation of the algorithm, Fig. 5 shows the normalized requested load and granted power for the case when microgrids 1, 2 and 3 were connected to buses 27, 29 and 30, respectively. The microgrids were intentionally located at neighboring buses in Area 1. Comparing Figs. 5a with 4a, it can be seen that during the 24 hours, the algorithm maintained almost the same grant to request ratio in Area 1, which has the highest priority. However, in Areas 2 and 3, the algorithm was not able to maintain the same grant to request ratio, as compared with the case in Fig. 4, since the majority of the loads were located in Areas 2 and 3. This introduced more losses, which limited the granted power. It can be also observed that the microgrid connected to bus 27

was always chosen to be the slack bus. This is due to the fact bus 27 has more connections to the other buses, as compared to buses 29 and 30, as shown in Fig. 1. Therefore, the line loading constraint eliminates the possibility of buses 29 and 30 to serve as the slack bus. It can also be noted that in this case, the total load requests were not granted during the off-peak hours, due to the location of the microgrids.

Similar to Figs. 2 and 3, Figs. 6 and 7 show the algorithm results for 7:00am and 9:00pm, respectively. It can be noted that the number of acceptable solutions in Fig. 6 and 7 is less as compared to Fig. 2 and 3, due to the fact that when either of buses 29 or 30 are chosen as the slack bus, none of the results yielded an acceptable solution in terms of line loading. It can be observed that Fig. 6 has more acceptable solutions as compared to Fig. 7, which represents the peak period. It should be noted that, in Figs. 6 and 7, some of the line loading and voltage results are outside the displayed range of y-axis.

Fig. 8 shows the voltage at the various buses for the 24 hours for the first case when the microgrids are connected to buses 3, 5 and 10. It can be seen that the voltage deviation increases during the peak hours, and that buses encounter the maximum voltage deviation. Since the algorithm selected the microgrid connected to bus 3 to serve as the slack bus for most of the day, the voltage at bus 3 is always close to 1 p.u.

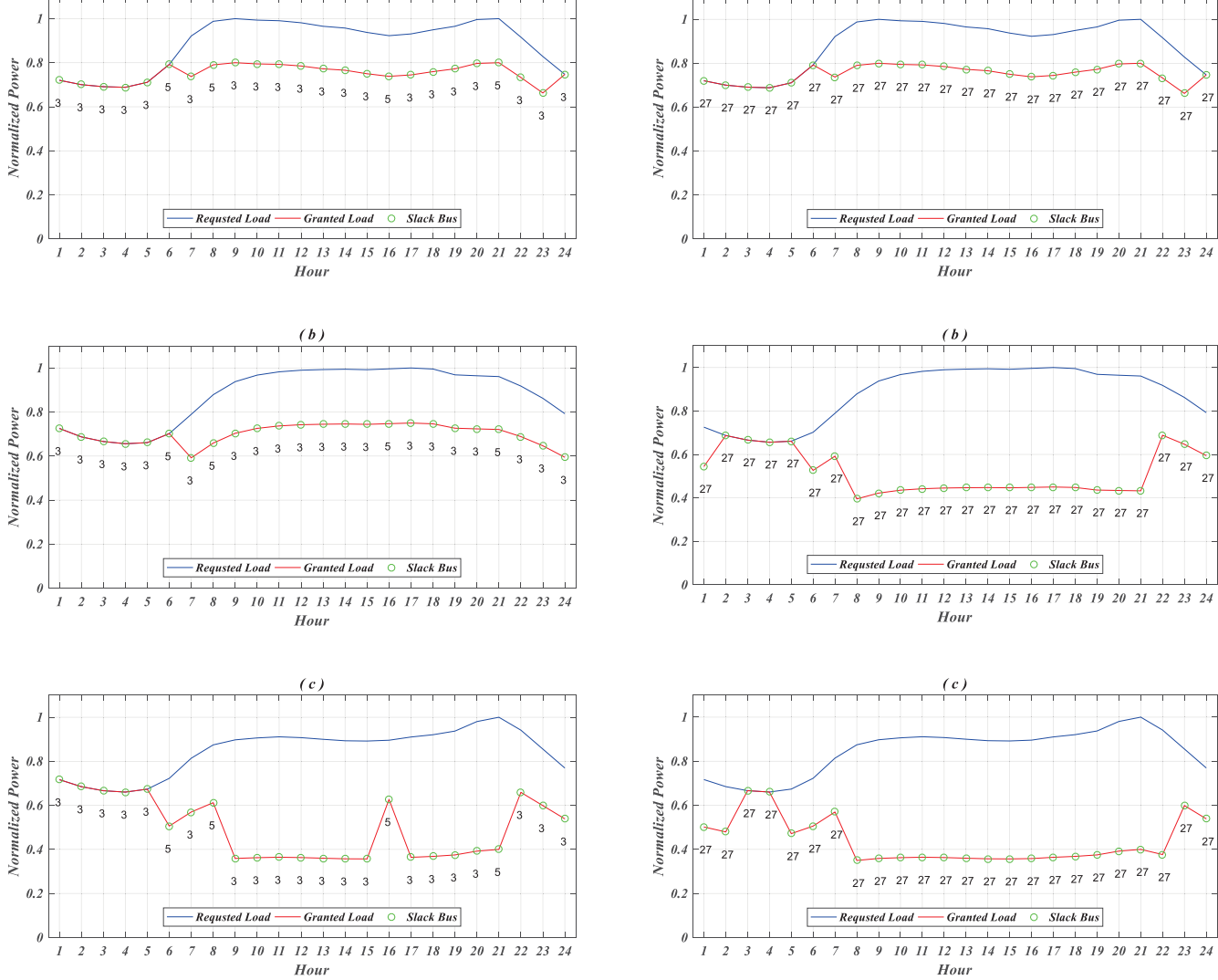


Fig. 4. Load request and granted power for 24 hours, with microgrids at buses 3,5 and 10, for: a) Area 1, b) Area 2 and c) Area 3.

Fig. 5. Load request and granted power for 24 hours, with microgrids at buses 27,29 and 30, for: a) Area 1, b) Area 2 and c) Area 3.

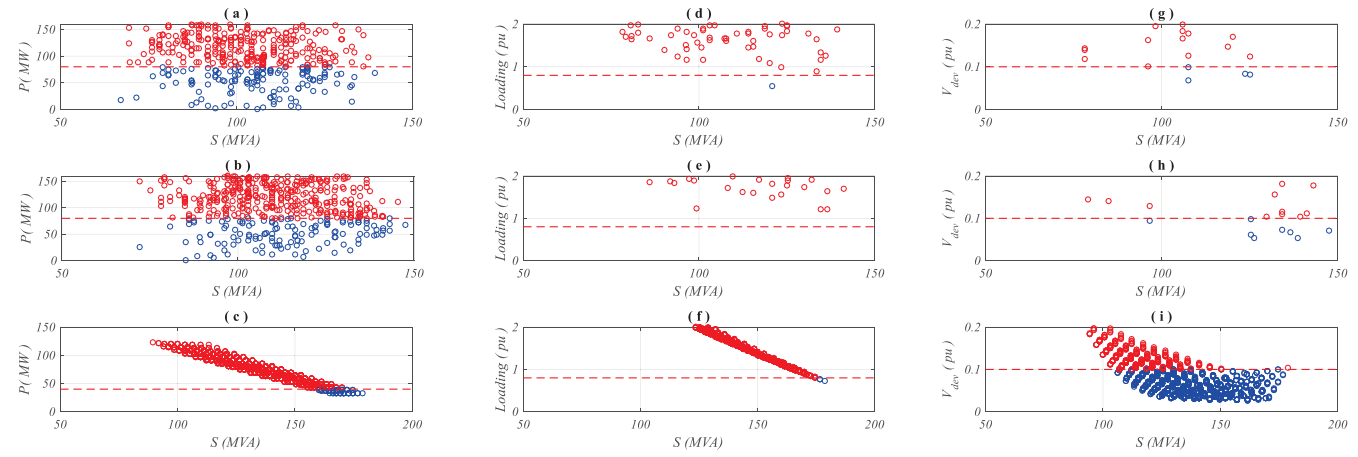


Fig. 6. Algorithm results at 7:00am, with microgrids at buses 27, 29 and 30.

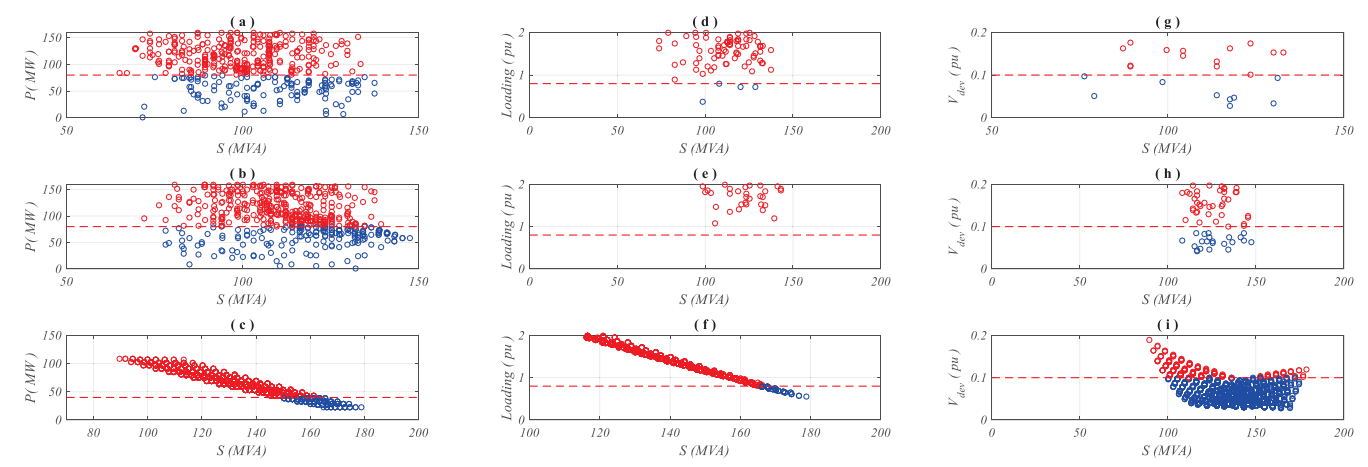


Fig. 7. Algorithm results at 9:00pm, with microgrids at buses 27, 29 and 30.

Figure 9 shows the progression of the algorithm as it goes through the various constraints. It can be seen that the algorithm starts with a large set of potential solutions, and then it converges to the optimal solution.

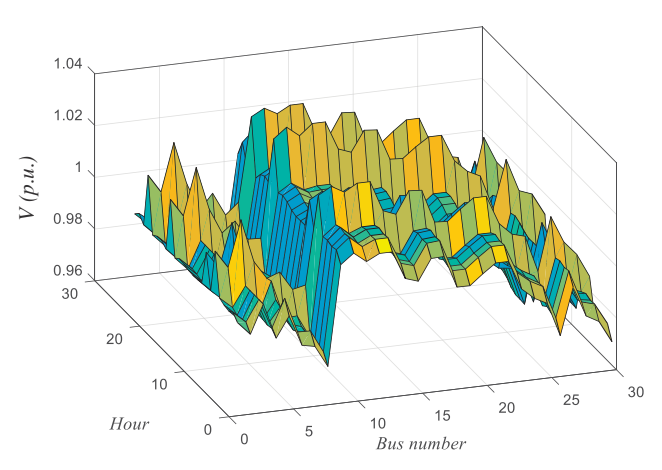


Fig. 8. Voltage variation at each bus during 24 hours, with microgrids at buses 3.5 and 10.

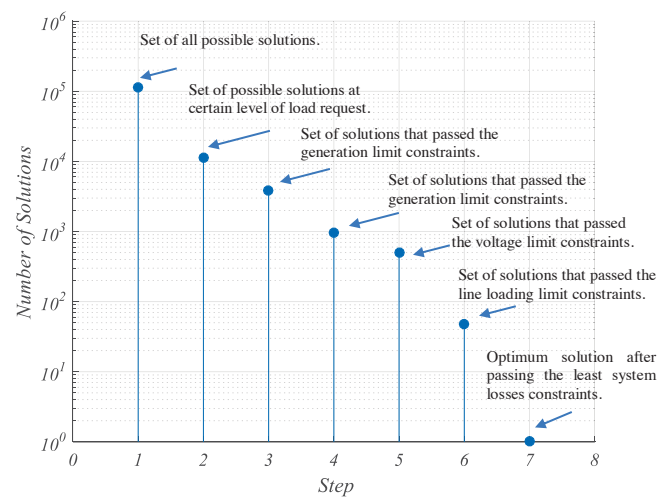


Fig. 9. Progression of the algorithm as it goes through the various constraints at 7:00am, with microgrids at buses 27, 29 and 30.

VI. CONCLUSIONS

In this paper, an energy management algorithm has been developed to enhance the resilience of electric power systems involving high penetration of microgrids, based on the Controlled Delivery Grid (CDG). The CDG concept suggests a radical change in the way electricity is delivered to end consumers. Loads have to send requests to the main controller, which may or may not grant them the requested energy based on the state of the power grid. Currently, the grid cannot cope with major disruption events. We have shown that by using power requests from the buses and by simulating the grid health ahead of actual power delivery, one can successfully minimize the risk of extended blackouts. The IEEE 30-bus Test Case has been used to examine the validity and applicability of the proposed algorithm. The developed algorithm aims at granting most of the load requests, while maintaining the voltage at each bus, line loading, and overall losses with acceptable limits. The results showed the feasibility of the proposed algorithm, and the potential of the CDG to enhance the resilience of the power grid.

REFERENCES

- [1] Available online at: https://obamawhitehouse.archives.gov/the-press-office/2013/02/12/presidential-policy-directive-critical-infrastructure-security-and-resil. Last accessed: 04/06/2017.
- [2] J. Duncan Glover, M.S.Sarma & Thomas J. overbye, "Power System Controls" in Power system analysis and design, 5th Edition, 2011, ch. 12, pp. 642-644.
- [3] "Electricity Advisory Committee," in http://energy.gov/, 2014. [Online]. Available: http://energy.gov/sites/prod/files/2014/10/f18/ModernizingElectricPowerDeliveryS ystem.pdf. Last accessed: 04/07/2017.
- [4] J. De La Ree, Y. Liu, L. Mili, A. G. Phadke, and L. DaSilva, "Catastrophic failures in power systems: Causes, analyses, and countermeasures," *Proc. IEEE*, vol. 93, pp. 956–964, 2005.
- [5] G. Andersson, P. Donalek, R. Farmer, N. Hatziargyriou, I. Kamwa, P. Kundur, N. Martins, J. Paserba P. Pourbeik, J. Sanchez-Gasca, R. Schulz, A. Stankovic, C. TaylorCauses and V. Vittal, "Causes of the 2003 Major Grid Blackouts in North America and Europe, and Recommended Means to Improve System Dynamic Performance", IEEE Transactions on Power Systems, Nov. 2005.
- [6] J. Kassakian, R. Schmalensee, W. Hogan, H. Jacoby and J. Kirtley, "The Future of the Electric Grid: An Interdisciplinary MIT Study," Massachusetts Institute of Technology, 2011. (Available online at: http://web.mit.edu/mitei/research/studies/the-electric-grid-2011.shtml).
- [7] GRIDWISE Alliance, "The Future of the Grid Evolving to Meet America's Needs," Western Region Workshop Summary, Prepared for the US Department of Energy by Enrgetic Incorporated under contract GS-10F-0103J.
- [8] Final Report on the August 14, 2003 Blackout in the United States and Canada: Causes and Recommendations. Available online at: https://energy.gov/sites/prod/files/oeprod/DocumentsandMedia/BlackoutFinal-Web.pdf. Last accessed: 04/06/2017.

- [9] R. Rojas-Cessa, Y. Xu and H. Grebel. "Management of a smart grid with controlleddelivery of discrete levels of energy." In IEEE Electrical Power and Energy Conference, 2013 IEEE International Conference on. IEEE, 2013, pp.1-5.
- [10] R. Rojas-Cessa, S. Vinit, M. Eugene, B. Divya, K. Justin and H. Grebel. "Testbed evaluations of a controlled-delivery power grid." In Smart Grid Communications (SmartGridComm), 2014 IEEE International Conference, 2014, pp. 206-211.
- [11] W. Shi N. Li C.-C. Chu R. Gadh "Real-time energy management in microgrids" IEEE Trans. on Smart Grid, 2015.
- [12] Pipattanasomporn M. Kuzlu M. and Rahman S. "An algorithm for intelligent home energy management and demand response analysis" IEEE Trans. Smart Grid vol.3 no.4 pp.2166-2173, Dec. 2012.
- [13] Y. Qu, H. Wang, S.-M. Lun, H.-D. Chiang, T. Wang "Design and implementation of a Web-based Energy Management Application for smart buildings" IEEE Electrical Power & Energy Conference, 2013.
- [14] E. Sortomme, M. M. Hindi, S. D. James MacPherson, S. S. Venkata "Coordinated charging of plug-in hybrid electric vehicles to minimize distribution system losses" IEEE Trans. Smart Grid vol. 2 no. 1 pp. 198-205, Mar. 2011.
- [15] H. S. V. Nunna; S. Battula; S. Doolla; D. Srinivasan" Energy Management in Smart Distribution Systems with Vehicle-to-Grid Integrated Microgrids" IEEE Trans. Smart Grid, pp 1-1, Dec. 2016.
- [16] K. Wang, Z. Ouyang, R. Krishnan, L. Shu, L. He "A game theory-based energy management system using price elasticity for smart grids" IEEE Trans. Ind. vol. 11 pp. 1607-1616, Dec. 2015.
- [17] Available online at: https://www2.ee.washington.edu/research/pstca/pf30/pg_tca30bus.htm. Last accessed: 04/06/2017.
- [18] Available online at: http://www.nyiso.com/public/markets_operations/market_data/graphs/index.jsp. Last accessed: 04/06/2017.